On the Robustness of Simple Indoor MANET Simulation Models

H. Andrés Lagar-Cavilla, Gerard Baron[‡], Thomas E. Hart,
Lionel Litty and Eyal de Lara

Department of Computer Science and
[‡]Department of Electrical and Computer Engineering
University of Toronto
andreslc@cs.toronto.edu

Abstract

We show that simple radio propagation and node mobility models widely used in MANET evaluation are not robust in indoor environments. Robust simulation models let researchers extrapolate simulation results and reach reliable conclusions about expected protocol performance. We experiment with two representative MANET routing protocols under different mobility and radio propagation models with decreasing levels of complexity. We show that the effects of successive simplifications to the node mobility and radio propagation models are not consistent across protocols. Moreover, even within the same protocol, the effects on performance can vary erratically as simulation parameters change. Our results raise troubling questions about the soundness of evaluations of MANET routing protocols based on simple radio propagation and node mobility models.

1 Introduction

A mobile multi-hop ad hoc network (MANET) consists of a group of mobile wireless nodes that self-configure to operate without infrastructure support. Nodes communicate information beyond their individual transmission ranges by routing packets over intermediate peers [1, 2, 3]. MANETS have been proposed for disaster relief operations, police and military applications, and other situations in which communication infrastructure is absent.

MANETs present formidable obstacles to evaluation. The mobile nature of nodes and the vagaries of radio propagation all but prevent reproducible experimentation in a controlled environment. It is therefore not surprising that the overwhelming majority of MANET research is evaluated using computer simulation [1, 2, 3, 4, 5, 6]. Simulation-based evaluation has many advantages:

it enables reproducible experiments in a controlled environment; it enables experimentation with large networks consisting of hundreds or even thousands of nodes; it enables researchers to experiment with configurations that may not be possible with existing technology; and finally, it allows for rapid prototyping.

The critical challenge for MANET simulators is to provide realistic models of radio propagation and node mobility. The radio propagation model determines, at a minimum, whether communication between two nodes is possible. The mobility model dictates how nodes choose destinations for their movement, the speed at which they move, and the physical paths they take.

The preeminent radio propagation and node mobility models used in MANET simulation are Free Space (FS) [7] and Random Waypoint (RWP) [4]. FS and RWP approximate large and open outdoor environments, devoid of obstacles. FS models propagation in an obstruction-free vacuum; signal strength degrades with the square of the distance between the transmitter and receiver. In RWP, a node picks a random destination inside a flat rectangular area, proceeds to it following a straight-line trajectory at a random speed, and pauses for a fixed time on arrival; the process then repeats.

We observe, however, that many scenarios for which MANET's have been proposed (e.g., search and rescue operations) take place in complex obstacle-rich indoor environments. Therefore, it is of crucial importance to carefully evaluate MANET protocols for indoor conditions.

This paper evaluates the *robustness* of simplified radio propagation and node mobility models for MANET evaluations in indoor environments. We define *robustness* of a simplified model as its ability to produce results consistent to those obtained with the original model under varied protocols and simulation conditions. A robust simplification allows researchers to extrapolate simulation results over different scenarios, and reach reliable conclusions about the expected performance of protocols in real life.

We conduct an experiment to determine the robustness of simplified simulation models for indoor MANET evaluation. The experiment compares the performance of DSR and DSDV, two representative MANET routing protocols, for two indoor environments under simulation models with different levels of detail and complexity. We first determine the performance of the two protocols under detailed site-specific radio propagation and node mobility models that account for fine-grained obstacles and building materials. We then observe the effects on protocol performance as we methodically reduce the complexity of the simulation models. The simplest models we consider correspond to the RWP and FS models commonly used in MANET evaluations.

Results from this experiment show that simplifications to the radio propagation and node mobility models are not robust. Simplifications to the simulation models have drastically different effects on the perceived performance of the two routing protocols. Whereas the performance of DSDV is unchanged across sim-

ulation models, DSR's performance varies widely between models. Moreover, within DSR itself, the relative performance across models changes erratically as we vary experimental parameters.

These findings raise doubts over the soundness of MANET evaluations based on simplified models. Because the effects of simplifications are not uniform across protocols and evaluation conditions, evaluation based on simplified models may lead researchers to reach incorrect conclusions about the performance of MANET protocols.

We present two main contributions: (i) we provide the first evaluation of MANET routing protocols in indoor environments using detailed node mobility and radio propagation models that account for fine-grained obstacles and building materials; and (ii) we show that widely used simplified node mobility and radio propagation models are not robust for (at least) indoor environments. Robustness is a qualitative measure of the adequacy of simulation models that – to the best of our knowledge – has not been identified or evaluated in previous work.

The rest of this paper is organized as follows. Section 2 describes our target environment and discusses the complexities of MANET simulation indoors. Section 3 and 4 discuss radio propagation and node mobility simulation models. In both sections, we first introduce a detailed model that accounts for fine-grained obstructions. We then present simplifications in which we gradually remove consideration of site-specific characteristics. Section 5 describes the experiment we conducted to evaluate the robustness of simplifications to the radio propagation and node mobility simulation models. Section 6 presents our experimental results. Finally, section 8 compares the paper to previous work on radio propagation and node mobility models, and section 9 concludes the paper and discusses future work.

2 Target Indoor Environments

Figure 1 shows the blueprints of our target environments, two academic research buildings at the University of Toronto. Figure 1(a) shows the 5^{th} floor of the Bahen Centre for Information Technology (*Bahen* for the rest of this paper), which stands on a 113 by 88 meter lot, and provides 5,400 square meters of living space. Figure 1(b) shows the 2^{nd} floor of the L. D. Pratt Building (*Pratt* for the rest of this paper), which stands on a significantly smaller area of 53 by 35 meters, and provides 1,225 square meters of living space.

Simulation of MANET protocols in indoor environments presents interesting challenges. Modern buildings can have irregular shapes and a large numbers of obstacles, which affect both node mobility and radio propagation. Figure 1 portrays the irregular layout of the buildings, but fails to convey a sense of their architectural complexity. In the case of Bahen, cement pillars, steel shafts, brick

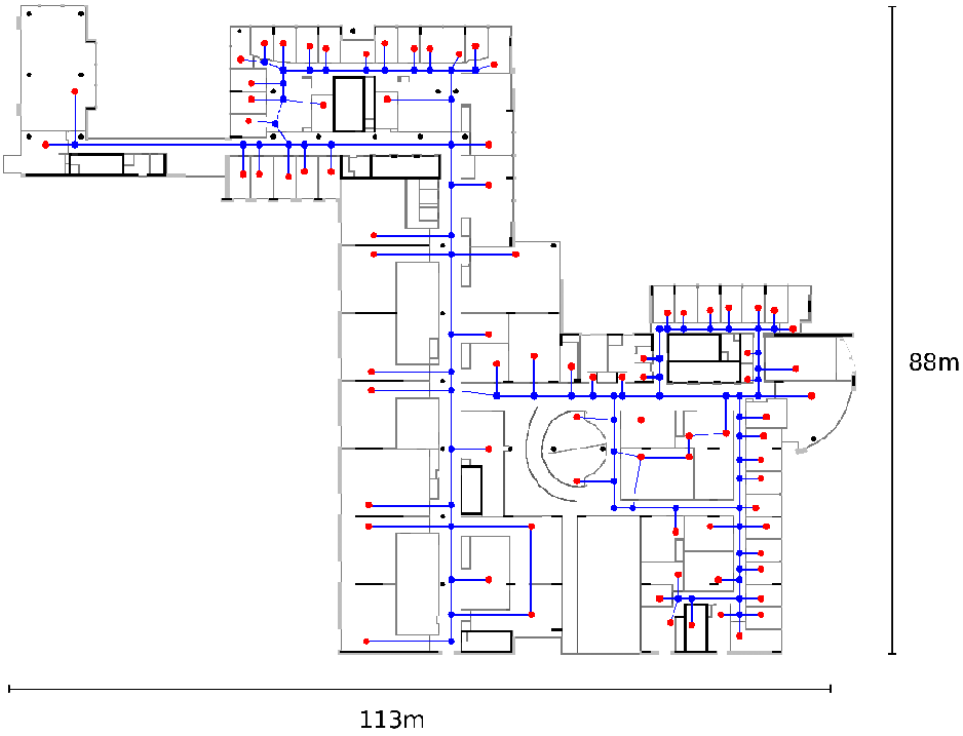

(a) Bahen

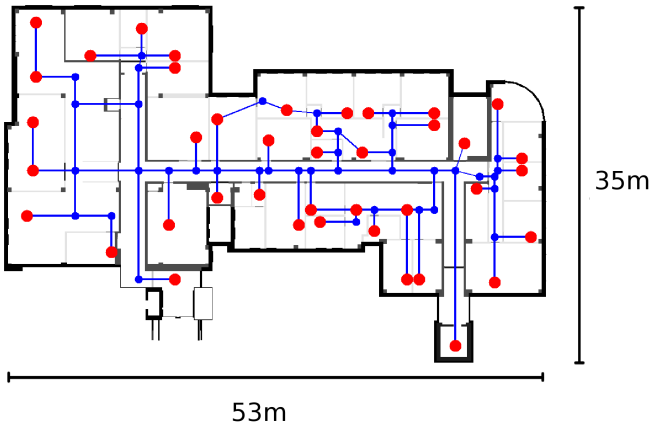

(b) Pratt

Figure 1: Target indoor environments.

walls, and the pervasive presence of glass are just some of its most relevant characteristics. Dating back a few decades, Pratt is representative of a more austere style, with a more regular layout and fewer and more traditional materials.

Moreover, buildings typically have multiple floors, adding a three-dimensional aspect to the simulation; movement between floors is possible using elevators and stairs. Indoor environments tend also to be much smaller than the outdoor scenarios traditionally considered in MANET research. For example, the area of Bahen or Pratt is at least two orders of magnitude smaller than what is usually considered in MANET simulations (e.g., a rectangular 1500 m $\times$ 300 m field space [4, 6]). Finally, because the environments under consideration are not ground floors, movement outside the floor plan is – for all practical purposes – impossible.

3 Radio Propagation Model

In this section, we first describe Attenuation Factor, a radio propagation model for indoor environments which accounts for obstacles and building materials. We then describe simplificastions to this model. We discuss all models in the context of single-floor simulation. Multi-floor extensions are left for future work.

3.1 Attenuation Factor

Attenuation Factor (AF) [7, 8, 9] is an empirical radio propagation model for indoor environments that deterministically accounts for multiple obstacles. AF models the attenuation of a transmitted signal as a function of distance and the effects of walls of different materials along the primary ray path, the straight-line between the transmitter and receiver. To the best of our knowledge, this is the first application of AF to MANET simulation; a fairly simplified version of AF has been employed by Bahl et al. [9] for location tracking.

AF models a time-invariant channel; it does not explicitly account for multi-path effects like reflection, diffraction, and scattering; and it does not take into account the thickness of obstacles. AF also assumes a two-dimensional topology and omni-directional antennas. Nevertheless, extensive practical experience has shown the model to yield good accuracy and high computational efficiency [7].

The AF model is given by eq. 1:

$$\bar{P}_{\mathrm{AF}}(r, m_1, ..., m_\sigma) = P_o(r_o) - 10n \log \frac{r}{r_o} - \sum_{i=1}^{\sigma} m_i \cdot \mathrm{PF}_i, \qquad (1)$$

where P_o is the power at some nearby reference distance r_o, n is the path loss exponent that determines the rate at which power decreases with distance r, m_i is the number of obstacles of material type i along the primary ray path,

PF_i is the partition factor loss due to material type i, and σ is the number of distinguishable material types.

The values for P_o, n, σ and the PF_is are site-specific empirical approximations derived from experimental measurements. We obtain the values for m_i from the floor plan, by counting the number of walls of various material types that intersect the primary ray path (whose length is r). The need for empirical signal-strength measurements is the fundamental source of overhead when implementing AF; runtime obstruction-detection adds little overhead with respect to simpler models such as FS.

We next describe the equipment used and methodology followed to derive these quantities for our target indoor environments.

3.1.1 Target Environment Parameterization

Our measurement platform consisted of two laptops running Linux equipped with Lucent Orinoco 802.11b network interface cards. The Orinoco cards were configured in ad hoc mode, and attached to a special external omni-directional antenna [10] that provided a gain of 9 dBi. The antennas also provided a horizontally-shallow (11 degrees of aperture) radiation pattern that minimized the effects of reflection on the floor and ceiling. At 2 Mbps, the Orinoco network interface has a nominal transmit power of 15 dBm, and a receive sensitivity threshold (for a Bit Error Rate $< 10^{-5}$) of -91 dBm [11]. With a cumulative gain of approximately 17 dB (two 9 dBi antennas minus pigtail losses), the setup was capable of recording receive signal strength values of -108 dBm for equivalent isotropic or unity gain (0 dBi) antennas.

We recorded 250 readings of signal strength in Bahen, and 150 measurements in Pratt. Each reading involved three steps. First, the two laptops were randomly positioned on different locations of the floor plan. Second, an attempt was made to establish communication between the two laptops. If successful, both laptops were configured to ping each other; otherwise, a new pair of locations was chosen. Finally, both laptops recorded signal strength values over a period of one minute; during which each made 30 measurements. We set the signal strength to the average of the measurements from both laptops.

We ran a regression test in MATLAB to obtain the site-specific values for P_o, n, σ and the PF_is . For each measurement point k we provided MATLAB with the recorded signal strength $\bar{P}_k$, the distance r_k from the transmitter, and the number of walls of each type m_{ik} between the transmitter and the receiver. r_o was nominally set to one meter. For Bahen, we could distinguish seven main material types in our AutoCAD floor plan: exterior walls, interior walls, exterior glass, interior glass, steel, concrete, and wood. For Pratt, the material count was six: brick walls, exterior walls, drywall, glass, wood and soundproof doors.

Table 1 lists the resulting parameterization of the AF model. For both floorplans, the best fit to the empirical measurements involved only four materials

Parameter	Bahen	Pratt
r_0 (m)	1	1
Num. of Materials	7	6
σ	4	4
P_0 (dBm)	-31.4627	-34.3944
n	1.9665	2.04998
PF_1 (dB)	2.479 drywall/wood	1.51269 glass/wood/doors
PF_2 (dB)	4.7727 steel/concrete	3.88813 drywall
PF_3 (dB)	3.11104 glass, both types	4.53147 brick
PF_4 (dB)	6.50076 exterior walls	2.4437 exterior walls
Av. Relative Error	8.8694 %	9.4932 %
Median Rel. Error	13.2806 %	7.9502 %
Rel. Error Std. Dev.	8.0745 %	8.0033 %

Table 1: AF parameterization for the two buildings under study.

classes (σ=4). The table lists the Partition Factor for each combination of materials, and the values for n and P_0, which account for the effect of furniture and smaller obstacles. On average, AF comes within 8.9% and 9.5% of the measured signal strength, for Bahen and Pratt, respectively.

Figure 2 shows the experimental data and the AF parameterization, for Bahen and Pratt. Each dot in the graph represents a reading from the experimental measurements, and each circle the corresponding AF approximation. In these two-dimensional graphs it is only possible to plot distance in meters vs. measured/predicted power in dBm; the notion of the different numbers of obstructing partitions attached to each data point cannot be accommodated. Figure 3 (a) shows AF-generated visualization of the signal strength for a transmitter placed in the center of the Bahen floor plan, and demonstrates the dramatic effect of wall attenuation on signal strength.

3.2 Radio Model Simplifications

We consider two simplifications to the AF model: Line-Of-Sight (LOS) and Site-Specific Free Space (FS′). LOS does away with the need for environment-specific measurements but retains the floorplan to identify obstructions. FS′ does away with the floorplan but requires environment-specific measurements.

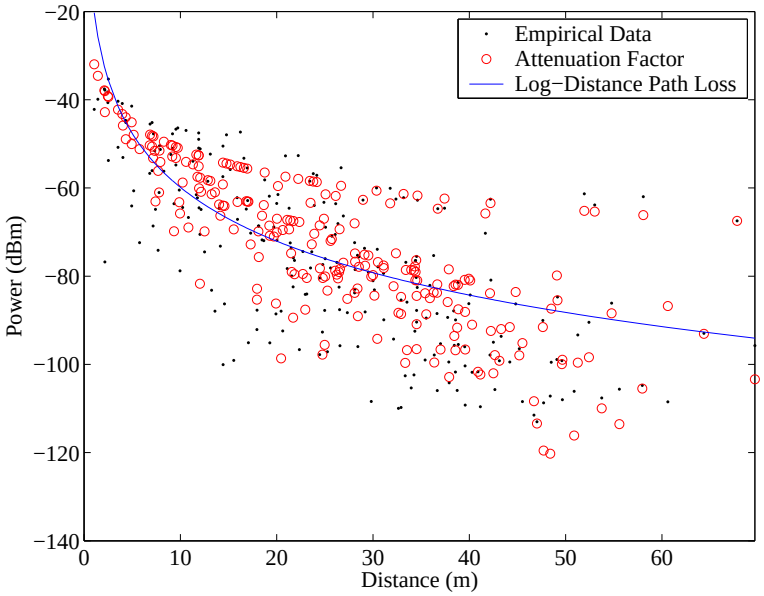

(a) Bahen

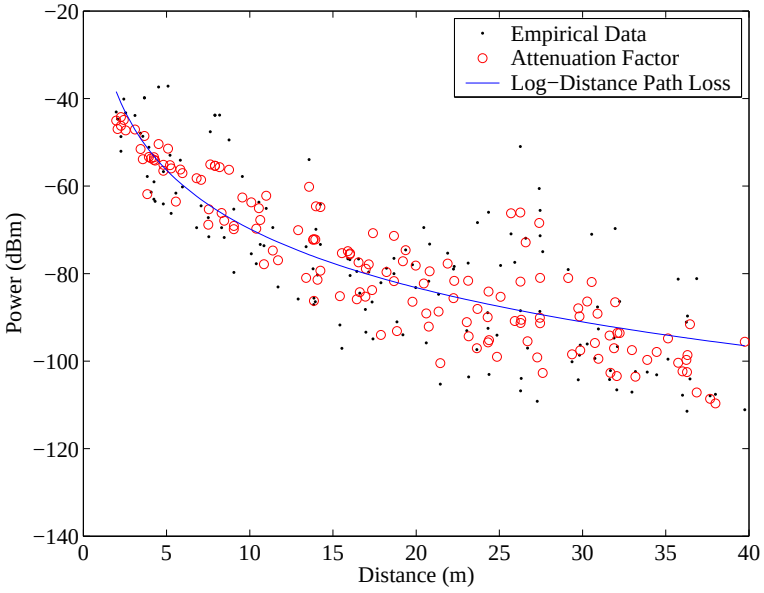

(b) Pratt

Figure 2: Signal strength measurements, and AF and PL fits.

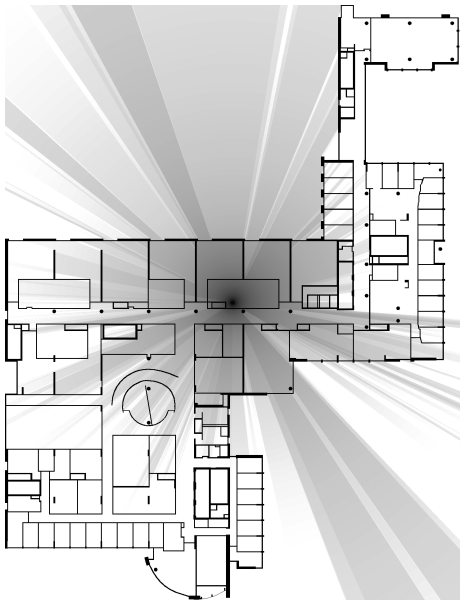

(a) AF

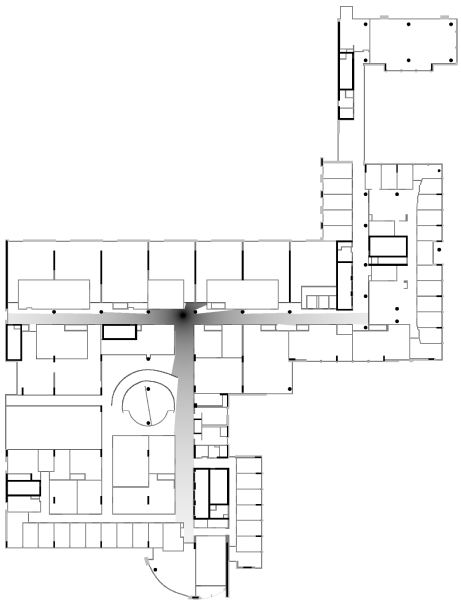

(b) LOS

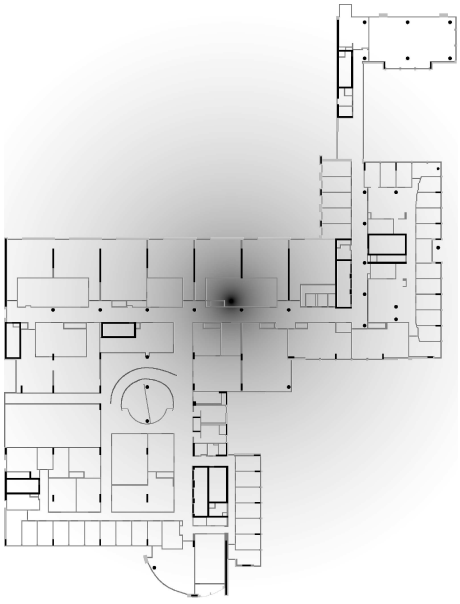

(c) FS'

Figure 3: Signal strength visualization under Attenuation Factor (AF), line-of-sight (LOS), and site-specific free space (FS').

3.2.1 Line-of-Sight

Line-Of-Sight (LOS) propagation assumes that communication is not possible whenever a wall intersects the primary ray path. In effect, LOS assigns infinite value to the PF_i's, and defaults to Free Space propagation when there is clear line of sight between the transmitter and receiver.

Figure 3 (b) shows a LOS-generated visualization of the signal strength for a transmitter placed in the intersection of two hallways in Bahen. Note how communication is only possible with nodes that are conveniently located in the same hallway.

3.2.2 Site-Specific Free Space

Site-Specific Free Space (FS′) removes the explicit consideration of obstacles. The Free Space (FS) model usually employed in MANET simulations is an extreme example of this approach, since it assumes that signals propagate though a vacuum. This is an inappropriate assumption for the indoor environments under study, as any single node will obtain full radio coverage of the network (e.g., default FS radio range in *ns2* is 250 meters). To obtain a realistic basis for comparison with AF, we employ the Log-Distance Path Loss (PL) function given by eq. 2:

$$\bar{P}_{\mathrm{PL}}(r) = P_o(r_o) - 10n \log \frac{r}{r_o} \tag{2}$$

PL is a generalization of FS. PL assumes propagation over an arbitrary homogeneous medium characterized by a path loss exponent n; in FS the vacuum medium has a path loss exponent $n = 2$. In turn, AF is a generalization of PL: if in the former we set all the PF_i's or σ to zero, we obtain the latter. The P_o and r_o components have the same meaning as in AF (eq. 1)

We used MATLAB to fit the PL equation to the empirical measurements taken in section 3.1.1. The resulting parameterizations are plotted in Figure 2 as solid lines. Table 2 shows the values used in the parametrization and provides error statistics for the fits. PL is significantly less accurate than the corresponding AF approximations.

Table 3 shows a set of AF sensitivity thresholds and the corresponding FS′ radio ranges. The sensitivity threshold is a hardware parameter that specifies the minimum signal-strength needed to successfully receive a packet; higher sensitivity thresholds are equivalent to lower transmitter power. The FS′ ranges are obtained by solving for r in eq. 2, with the specified sensitivity threshold on the left-hand side and the parameters from table 2 on the right-hand side. The obtained radio ranges offer a reasonable basis for comparison to AF and reveal fundamental characteristics of each building. Bahen's modern architectural layout, characterized by large open spaces, wider hallways, and the use

Parameter	Bahen	Pratt
r_o (m)	1	1
P_0 (dBm)	-19.2464	-25.1998
n	4.0602	4.4578
Average Relative Error	14.847 %	12.931 %
Median Rel. Error	13.291 %	10.162 %
Rel. Error Std. Deviation	11.4 %	12.129 %

Table 2: PL parameterization for the two buildings under study.

AF Threshold (dBm)	-51	-61	-71	-81	-91
FS′ Range Bahen (m)	6.1	10.7	18.8	33.2	58.5
FS′ Range Pratt (m)	3.8	6.4	10.7	17.9	29.9

Table 3: FS′ effective ranges for AF thresholds.

of "softer" building materials such as drywall (as opposed to brick in Pratt), yields an environment more conducive to radio propagation. As a result, for the same transmitter power, effective radio ranges for Bahen are practically twice as large as those in Pratt.

4 Node Mobility Model

In this section, we first describe a detailed node mobility model for indoor MANET simulation that accounts for obstacles. We then present simplifications to this model. As was the case in the previous chapter, all models are limited to single-floor simulations. Extensions to multi-floor simulations are the subject of future work.

4.1 Constrained Mobility

The Constrained Mobility (CM) model uses a *mobility graph* to constrain node movement by the obstacles present in the environment. For example, Figure 1 shows mobility graphs superimposed over the floorplans of the Bahen and Pratt buildings. Vertices represent possible destinations that nodes can visit, and edges correspond to physically-valid paths over which nodes can move toward their intended destinations. Movement from one destination to another is accomplished by traversing the edges that constitute the shortest path between the two corresponding vertices. Therefore, nodes use doors and hallways to reach their destinations.

We limit the choice of destinations to vertices in the graph situated in "interesting" locations such as offices, classrooms and conference rooms. Each node randomly chooses a vertex in this set, and moves toward it at a randomly selected speed. After reaching its destination, the node pauses for a random period of time. This process then repeats itself. Constrained mobility is modular to behavioral considerations explored in other mobility models. CM can be improved by adding any of the behavioral models approaches explored in recent MANET mobility research [12, 13, 14].

At present, we draw the mobility graph on top of the floor plan (and identify the set of interesting locations) using a simple graphical editor we developed. We use existing AutoCAD drawings, so this is not a laborious task. Moreover, the mobility graph needs to be built only once for a given floor plan, and is then reused in a large number of simulations. Nevertheless, we plan to explore techniques to automate the generation of mobility graphs.

4.2 Mobility Model Simplifications

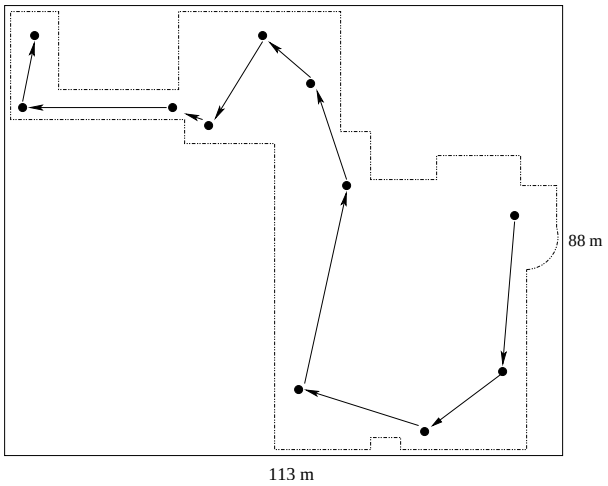

Figure 4: Shell mobility model, Bahen.

We present three simplifications to Constrained Mobility that gradually remove the consideration for site-specific characteristics.

4.2.1 Shell

The CM model described above takes into account both internal and external walls. *Shell* discards the internal walls of the building and the mobility graph. In Shell, nodes select destinations randomly within the area outlined by the

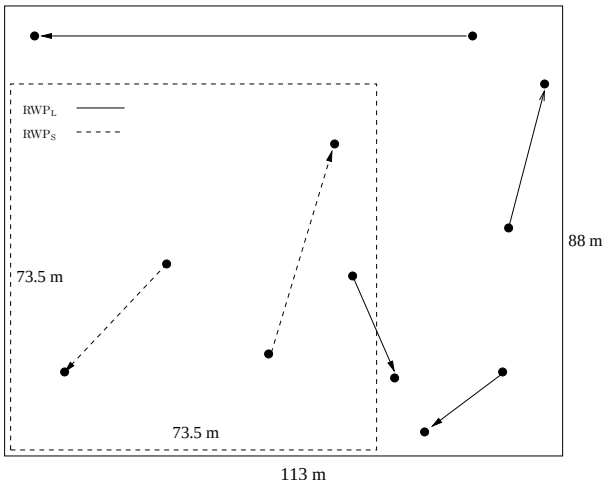

Figure 5: RWP mobility model, Bahen.

external walls of the building, and follow straight-line paths to their destinations. Shell thus increases the number of possible destinations, and distributes them uniformly. However, choice of destinations is constrained to locations that will not force nodes to step outside of the floor plan perimeter. Figure 4 illustrates the Shell mobility model.

4.2.2 Random Waypoint (RWP)

Discarding the external walls from the Shell model yields the Random Waypoint (RWP) [4] model. We consider two variants of RWP. In the RWP_S (*small*), nodes move inside a square with an area equivalent to that of the Shell and CM models. In RWP_L (*large*), nodes move in a rectangle whose area is that of the lot over which the building stands. For Bahen, the RWP_S area is a square with 73.5 meter sides, and the RWP_L area is a rectangle of 88 by 113 meters; for Pratt, the RWP_S area is a square with 35 meter sides, and the RWP_L area is a rectangle of 53 by 35 meters. Figure 5 illustrates the two RWP variants for Bahen.

5 Experiment

In this section, we describe the experiment we conduct to assess the robustness of simplified simulation models for evaluating MANETs in indoor environments. Our experiment compares the simulated performance of DSR [1] and DSDV [2], two representative MANET protocols, under different node mobility and ra-

dio propagation models. Initially, we determine the performance of DSR and DSDV under site-specific mobility and radio propagation models that account for fine-grained obstacles and building materials. We then observe the effects on protocol performance as we methodically reduce the complexity level of the simulation models. The simplest models we consider correspond to the Random Waypoint and Free Space mobility and radio propagation models used in most MANET evaluations.

Specifically, we consider six combinations of the mobility and radio propagation models described in sections 3 and 4. We asses the robustness of simplifications of the radio propagation model by comparing the performance of DSR and DSDV under Constrained Mobility with Attenuation Factor (CM-AF), with that obtained under Constrained Mobility with Line-Of-Sight (CM-LOS) and site-specific Free Space (CM-FS′). Similarly, we asses the robustness of simplifications of the mobility model by comparing the performance of the protocols under CM-FS′ to that under Shell and Random Waypoint with site-specific Free-Space propagation (Shell-FS′ and RWP-FS′). For Random Waypoint, we consider both RWP_S-FS′ and RWP_L-FS′, which correspond to the livable area and rectangular dimensions of a building, respectively.

In the rest of this section we first describe DSR and DSDV, the two MANET protocols that we used in our evaluation. We then describe our experimental environment. Section 6 presents the results of the experiment.

5.1 MANET Routing Protocols

MANET routing protocols can be characterized as reactive or proactive. Reactive, or on-demand, routing protocols only update routes when packets need to be transmitted along them, while proactive protocols attempt to keep up-to-date routing tables at all times, irrespective of traffic patterns. We next describe DSR [1] (on-demand) and DSDV [2] (proactive), two widely used MANET routing protocols that we use in our experiment. We chose these protocols as they represent "pure" extremes in the design space.

5.1.1 Dynamic Source Routing (DSR)

DSR is an on-demand source routing protocol. DSR has two operation modes: *route discovery* and *route maintenance*. Whenever a node sends a packet, DSR first checks its local cache for a route to the destination. If DSR finds a route, it inserts the route into the packet and forwards the packet toward its destination. If no route is found, DSR switches to route discovery mode and broadcasts a route request packet. On receiving a route request packet, a node appends itself to the source route in the packet, and either (i) identifies itself as the destination by sending a route reply to the source via a reversed source route, or (ii) rebroadcasts the route request packet. On receiving the route reply, the

source node adds the route to its cache and forwards the data packet along the newly acquired source route. Route discovery may result in many route responses (multiple routes to a destination). These source routes are cached by DSR and the shortest source route is used.

Route maintenance is DSR's standard operation mode. While in route maintenance, DSR routes data packets using the source route. On receiving a data packet, a node unicasts the packet to the node listed as the next hop in the source route. Whenever a packet fails to be sent to its next hop, DSR assumes the link is broken, cleanses its cache of routes using the link, and sends a unicast *route error* message to the packet original sender, who attempts to find a new route to the destination node in its cache. If no route is found, the sender switches to the route discovery mode.

DSR includes several mechanisms that attempt to reduce the significant cost associated with route discovery operations. For example, intermediate nodes in DSR can cache overheard routes and respond to route requests for which they have cached source routes. Other optimizations include salvaging, where intermediate nodes attempt to salvage a packet by retransmitting it over an alternative route when the provided source route fails, and expanding broadcast rings, where an initial route discovery message is broadcast only to the node's immediate neighborhood. When no route is found among the immediate neighbors, a regular route discovery broadcast follows.

5.1.2 Destination Sequence Distance Vector (DSDV)

DSDV is a table-driven proactive routing protocol, that builds on the Bellman-Ford distance-vector routing algorithm [15]. Every node keeps a routing table (the distance vector) with entries for all other nodes in the network. A routing entry includes the destination's address, the next hop to the destination, a metric (usually the path length), and a sequence number to indicate the freshness of the information, and to ensure loop-free routing. Nodes exchange full routing table contents periodically (typically every 15 seconds). Nodes can also produce an unscheduled or triggered update upon learning of a shorter or fresher route. Triggered updates only contain affected distance vector entries, and their rate of generation is regulated through a set of timing constraints.

5.2 Experimental Environment

We conducted our experiments using the *ns2* [16] network simulator version 2.26 with the CMU wireless extensions [17]. We used the *ns2* implementations of the 802.11 DCF MAC protocol, and the DSR and DSDV routing protocols. The channel's capacity and frequency were 2 Mbps and 2.4 GHz, respectively.

We extended *ns2* with the AF propagation model using eq. 1 and the empirical parameters derived in section 3.1. Our AF implementation can compute

Parameter	Values
Indoor environments	5^{th} floor Bahen 2^{nd} floor Pratt
Simulation models	CM-AF, CM-LOS, CM-FS′, Shell-FS′, RWP_S-FS′, RWP_L-FS′
Protocols	DSR, DSDV
Simulation time	1200 sec
Nodes	20, 30, 40, 50
Radio range	AF: -51 to -91 dBm FS′: 5 to 60 meters (Bahen) 5 to 30 meters (Pratt)
Traffic	CBR, 64 bit pkt, 4 pkts/sec
Traffic sources	10, 15, 20 ,25
Node speed	0.5 to 3 meters/sec

Figure 6: Experimental parameters.

signal strength at the receiver for any pair of nodes arbitrarily positioned inside the modeled floor plan. We determine the number of walls in the primary ray path, and their material types, by computing the intersections between the primary ray and the building's geometry captured in the AutoCAD floor plan. To generate CM and Shell mobility patterns, we developed extensions to the *setdest* program that incorporate the mobility graph and floor plan shape specifications as additional inputs. We instantiated our models for two indoor environments: the 5^{th} floor of the Bahen Centre for Information Technology (Bahen) and the 2^{nd} floor of the L. D. Pratt Building (Pratt). All extensions, along with additional data generation and analysis tools, are freely available under the GPL license at the author's website [18].

Table 6 summarizes the evaluation parameters. We report results for networks of 30, 40 and 50 nodes. We also ran simulations for networks of 20 nodes, but we do not include there results as they are virtually identical to those of the 30 nodes network. In all simulations, nodes choose a speed uniformly distributed between 0.5 and 3 m/s, which we regard as the range of human walking speeds in an indoor environment; in particular, we chose a non-zero minimum speed to avoid the average speed decay phenomenon analyzed in [19]. To stress the network, we set the pause time to zero.

We experimented with a variety of sensitivity thresholds for the AF model, ranging from the default -91 dBm up to -51 dBm, with a step of 10 dBm. Based on the mappings from Table 3, we experimented with FS′ effective ranges between 5 and 60 meters for Bahen, and 5 and 30 meters for Pratt. For LOS propagation, we only experimented with the largest of the mentioned radio

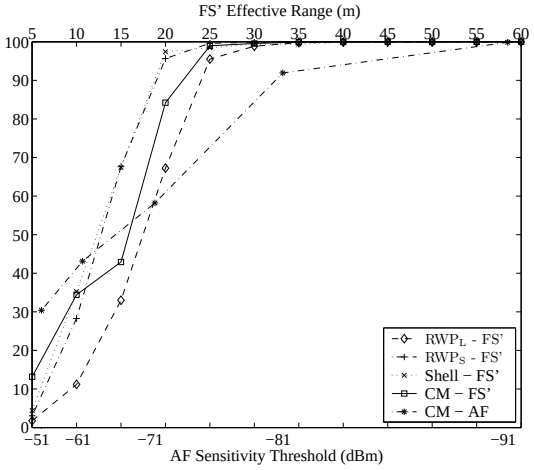

(a) 40 Nodes

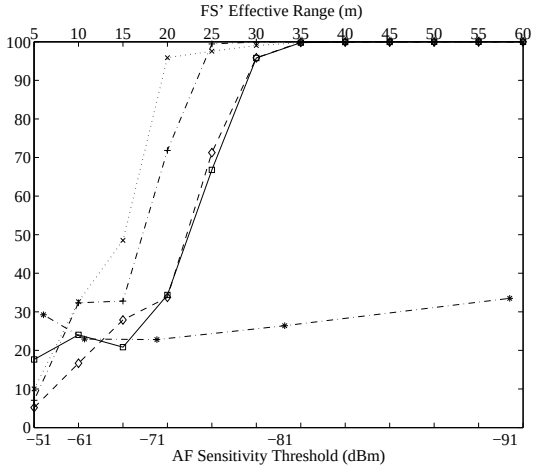

(b) 30 Nodes

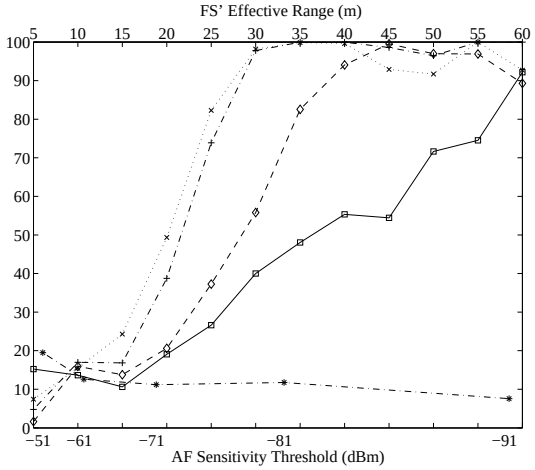

(c) 50 Nodes

Figure 7: DSR packet delivery rate, Bahen.

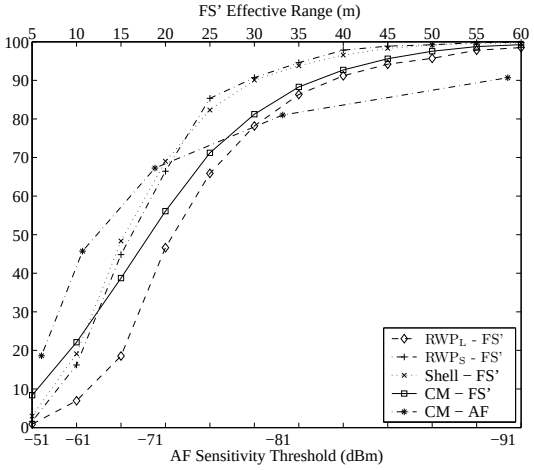

(a) 40 Nodes

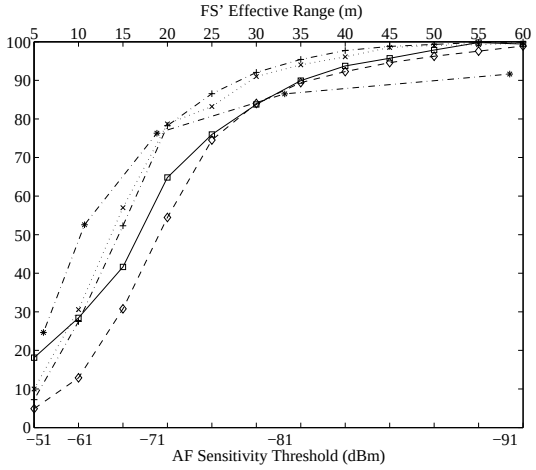

(b) 30 Nodes

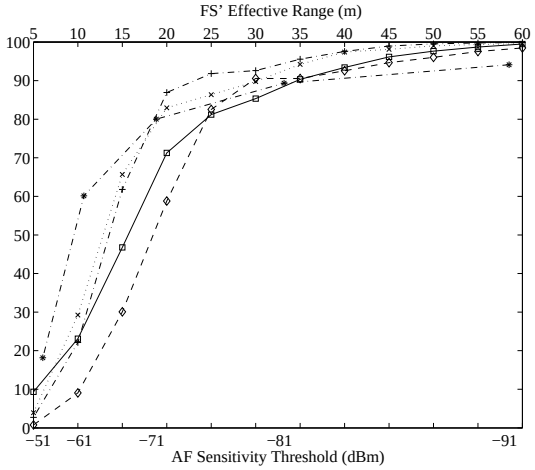

(c) 50 Nodes

Figure 8: DSDV packet delivery rate, Bahen.

ranges for each building.

We modeled network traffic using Constant Bit Rate (CBR) sources. In each experiment, half the nodes in the network are CBR sources, and each source transmits 64-byte packets at a rate of 4 per second. Sources are randomly paired with receivers at the start of the simulation and these parings are maintained for the length of the simulation. We chose these parameters to match the settings used in other studies of MANET routing protocol performance [4, 5, 6], and thus simplify result comparison. However, we also experimented with different sending rates, packet sizes and number of sources; we do not include those results as they show similar trends.

All results are averages of five runs over different randomly generated mobility patterns. No significant variance was observed among different runs for the same scenario; standard deviation values were consistently smaller than 10% of the corresponding average. All experiments ran for 1200 seconds of simulated time.

6 Results

In this section, we present results for the experiments conducted with DSR and DSDV under different node mobility and radio propagation simulation models. Our objective is not to determine which MANET protocols is the best performer. Instead, we explore the robustness of simplifications to the node mobility and radio propagation models, and the effects (if any) that these simplifications have on the evaluation of MANET routing protocols.

The rest of this section is structured as follows. We first evaluate the robustness of simplifications to the node mobility and radio propagation models by comparing the packet delivery rate (PDR) of DSR and DSDV under different simulation models. With the aid of two simple examples, we then show how the lack of robustness of the simple simulation models can lead researchers to reach incorrect conclusions. We then explain the differences in protocol performance between simulation models by looking at the effect the simulation models have on the rate of network topology change. Finally, we reflect on the implication and reach of our results and provide high-level recommendations for MANET routing protocol design.

6.1 Robustness

Figures 7 and 8 show the Packet Delivery Rate (PDR) of DSR and DSDV for networks of 30, 40 and 50 nodes in Bahen. Figures 9 and 10 show results for DSR and DSDV in Pratt. All figures have two scales on the x axis. The bottom scale shows receiver sensitivity in dBm, applicable to the experiments

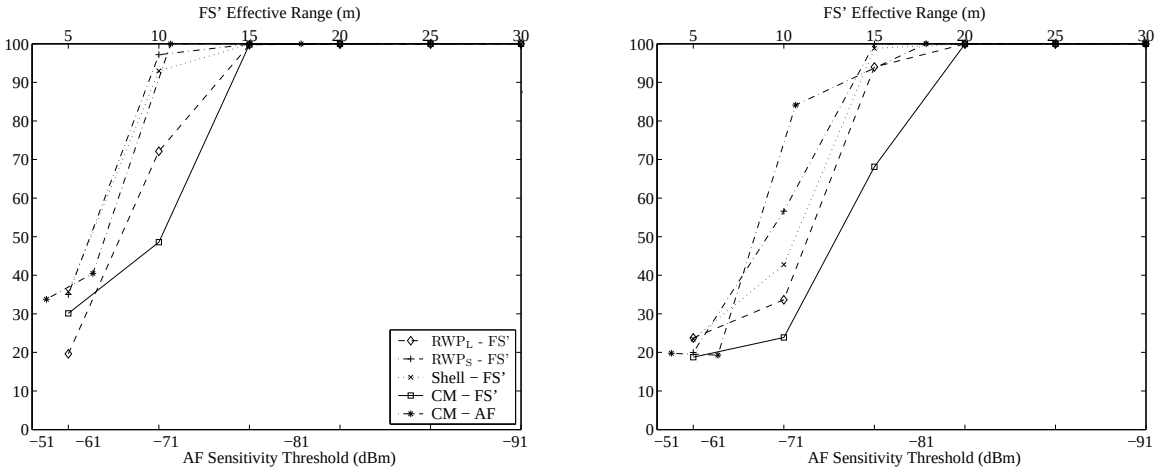

(a) 40 Nodes

(b) 30 Nodes

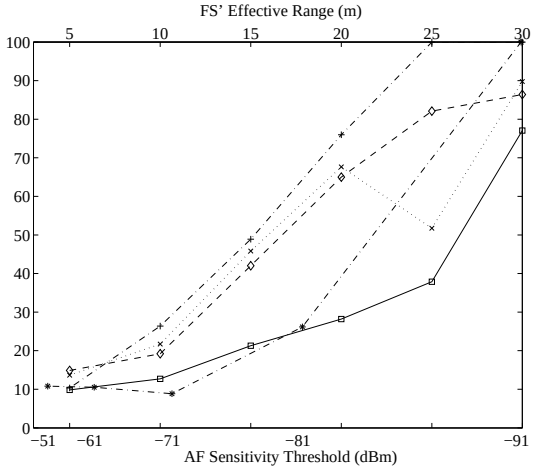

(c) 50 Nodes

Figure 9: DSR packet delivery rate, Pratt.

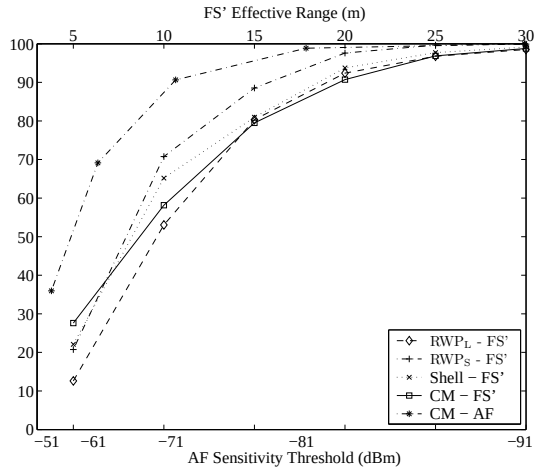

(a) 40 Nodes

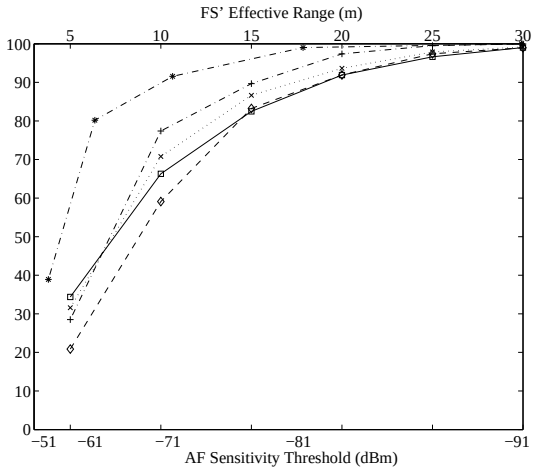

(b) 30 Nodes

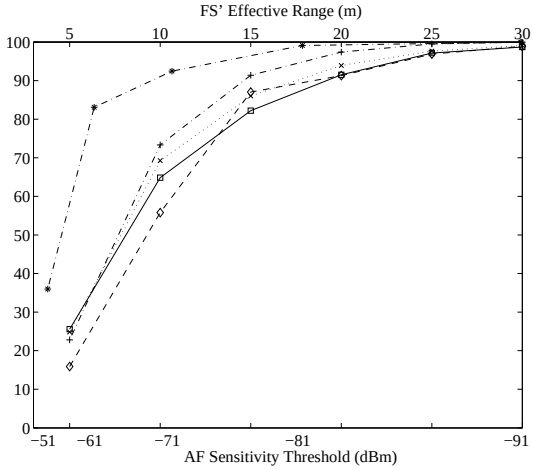

(c) 50 Nodes

Figure 10: DSDV packet delivery rate, Pratt.

run under Attenuation Factor (AF). The top scale shows site-specific transmission range in meters, applicable to the experiments employing site-specific Free Space (FS′). Section 3.2 describes how we determine the site-specific mappings between receiver sensitivity and transmission range.

Figures 7-10 do not include results for CM-LOS because PDR for both DSR and DSDV was always bellow 30%. Communication in CM-LOS is only possible when nodes are located on the same hallway or intermediate nodes are conveniently located in a hallway intersections. Based on the low PDR, we conclude that LOS is too restrictive and is not an appropriate radio propagation model for indoor environments.

A first indication that simplifications to the simulation models may not be robust can be seen by comparing the performance of DSDV and DSR in both Bahen and Pratt (Figs. 7 vs. 8 for Bahen and Figs. 9 vs 10 for Pratt): the effects of the simplifications on performance are not uniform across the two protocols. While successive simplifications do not alter the performance of DSDV, the performance of DSR changes dramatically across models. This is an indication that conclusions reached about the relevance of detail for MANET evaluation may not carry over across protocols. The DSR results (Fig. 7 and 9) provide a second indication that simplified models may not be robust: the performance of DSR across models changes dramatically as we increase the number of nodes. The implication is that observations about the relevance of detail do not necessarily carry over even within the evaluation of the same protocol as we change the experimental parameters.

Interestingly, the DSR results for the 50 nodes' network in Pratt (Fig. 9 (c)) show a sudden increase in performance for CM-AF, as receiver sensitivity reaches -91 dBm. This is in pronounced contrast with the results obtained under the same conditions in Bahen (Fig. 7 (c)). As we will show in section 6.4, when nodes transmit at full power in Pratt, they attain almost complete building coverage; for CM-AF, a node can reach directly 86% of its peers in average. Thus, for most communicating pairs, the network becomes single-hop, bypassing the multi-hop routing protocol altogether. We further discuss the effects of the simulation model on network topology in section 6.4.

Based on the DSR results we observe that: (i) there is significant difference in the performance of DSR between CM-AF and CM-FS′, a strong indication that the sophistication of the radio propagation model can affect the results of the evaluation; (ii) there are differences in the delivery rates of DSR under CM-FS′ and Shell-FS′, an indication that internal walls can affect the results of the evaluation even when they only limit mobility, and do not affect radio propagation; and (iii) it appears that DSR Shell-FS′ and RWP_{S}-FS′ are equivalent mobility models, and that therefore external walls have much less of an effect on the simulation results than the internal walls.

6.2 Implications for MANET Evaluation

In this section we illustrate the implications of the lack of robustness of simplified radio propagation and node mobility simulation models. Specifically, we provide two examples of how evaluations based on simplified models may lead researchers to reach erroneous conclusions.

Our first example illustrates pitfalls due to the lack of robustness in simplifications to the node mobility model. Assume that we are evaluating an energy-aware optimization to DSR that extends battery life by reducing transmitter power at all nodes to the same lower level. Assume that based on the DSR results for the 30 nodes network in Bahen (Figure 7 (a)), we were to (wrongly) conclude that both Shell-FS′ and RWP_S-FS′ are good approximations of CM-FS′. Evaluation of this optimization under Shell-FS′ or RWP_S-FS′ would lead us to the erroneous conclusion that for a 50 nodes' network a transmission range of 35 meters (roughly a 10 dBm transmit power reduction) achieves a delivery rate close to 100%. However, this is not the case for the more sophisticated CM-FS′ model, which reveals that only half of the packets will be successfully delivered (Figure 7 (c)); therefore, the power adaptation policy will not be effective for this network.

The second example considers simplifications to both the radio propagation and mobility model. Assume that we are performing a comparative study of the performance of DSDV and DSR. Further, assume that based on the DSDV results we were to (wrongly) conclude that RWP_L-FS′, a simple model which assumes no obstacles for mobility or radio propagation, is a good approximation of the more complex CM-AF. The similar performance curves of both models, and the fact that the results obtained with RWP_L-FS′ are within a bounded and consistent error from the results of the sophisticated model, substantiate this hypothesis. Unfortunately, if we evaluated DSR using RWP_L-FS′, we would reach the erroneous conclusion that DSR matches or even outperforms DSDV in this environment. Note that the exact opposite occurs with the more detailed model.

6.3 Simulation Model Effects on Network Topology

To explain the differences in protocol performance between simulation models, we look at how the simulation model affects routing overhead. Figures 11 and 12 show the number of routing packets for DSR and DSDV in Bahen. Results for Pratt (not included) show similar trends. For DSR there is a large divergence in routing overhead between the models (note the logarithmic scale used in the graphs). This difference becomes more significant as the network grows in size. In contrast, for DSDV there is little variation between the models, and the overhead increases modestly with the number of nodes. We conclude that poor DSR performance under CM-AF and CM-FS′ results from the overwhelming

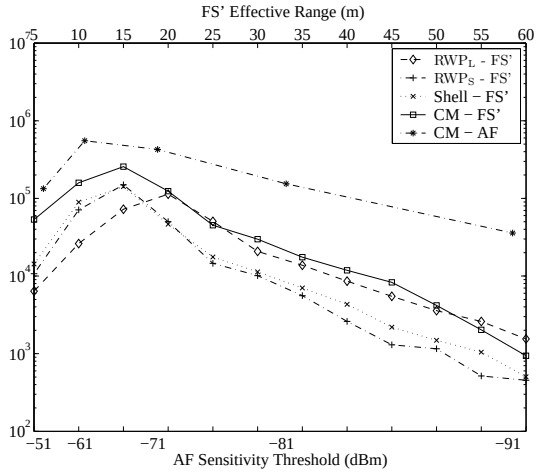

(a) 40 Nodes

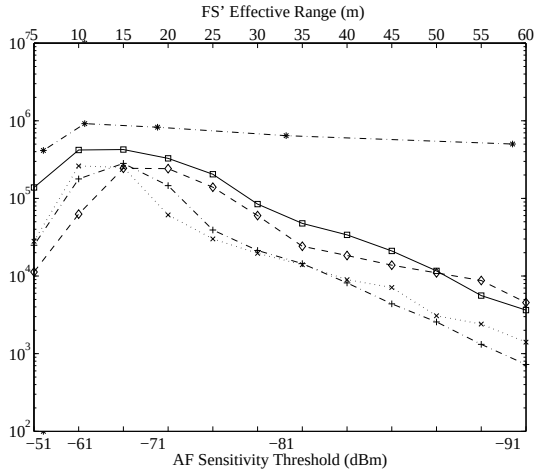

(b) 30 Nodes

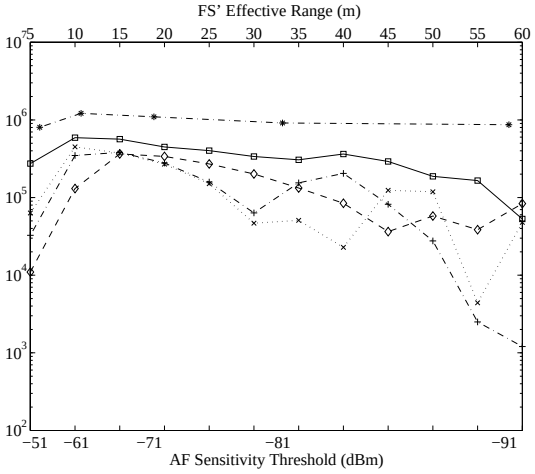

(c) 50 Nodes

Figure 11: DSR routing packets overhead, Bahen.

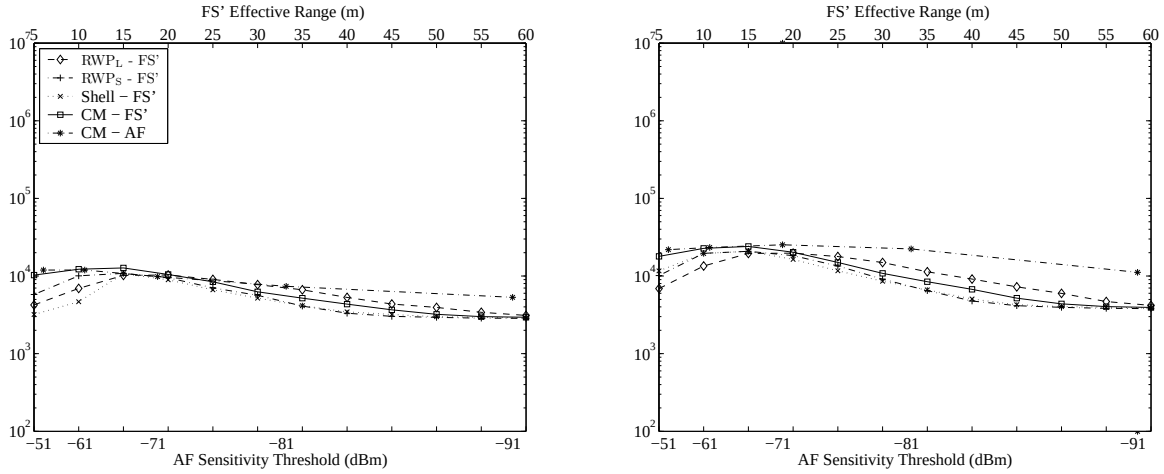

(a) 40 Nodes

(b) 30 Nodes

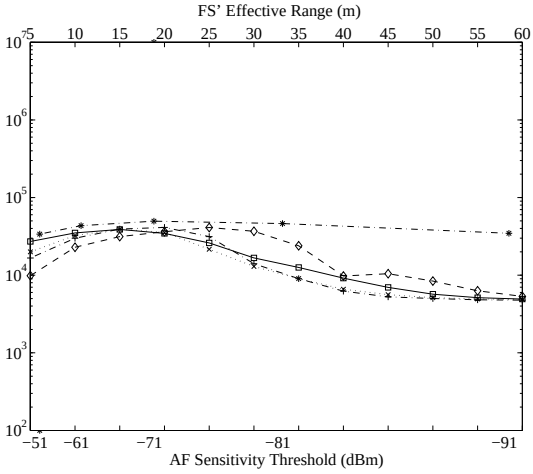

(c) 50 Nodes

Figure 12: DSDV routing packets overhead, Bahen.

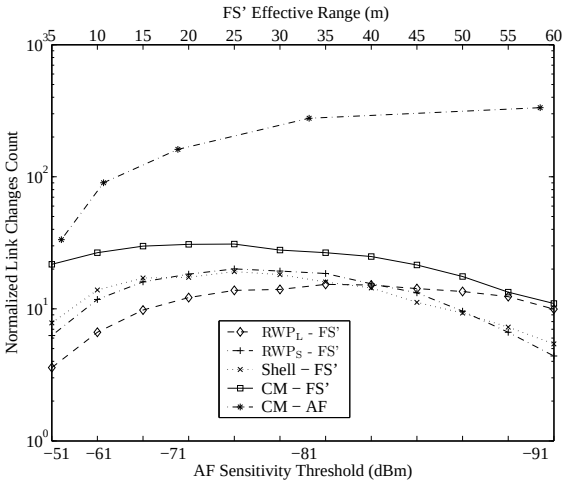

Figure 13: Normalized link changes, Bahen

increase in routing overhead.

We attribute the large differences in DSR routing overhead to the effects the simulation models have on the rate of topology change. To characterize such rate we employ metrics that are independent of communication patterns (i.e., they do not depend on network traffic or the routing protocol). The metrics depend only on the mobility and radio propagation models, and the length of the simulation.

Figure 13 shows the normalized number of link changes for a network of 40 nodes in Bahen. The number of link changes increases by one every time that two nodes that are within radio range go out of range, or vice versa. We normalize the total number of link changes by the total number of possible links, $n * (n-1)/2$ (with n being the number of nodes). Because of normalization, results for 30 and 50 nodes (not shown) are essentially identical. Figures 14 and 15 display the cumulative distribution of disconnection times for a network of 40 nodes in Bahen. Disconnection time measures the length of the interval for which two nodes remain out of the radio range of each other. Results for networks of 30 and 50 nodes (not shown) are similar.

Figure 13 shows that there is a large difference in the number of link changes between CM-AF and CM-FS′ (note the logarithmic scale). In CM-AF, radio connectivity changes abruptly as nodes move behind obstacles. Figure 14 shows that the majority of disconnections in AF propagation are short-lived; most of the link breakages (close to 90 % with a sensitivity threshold of -91 dBm) last less than one second. Interestingly, as receiver sensitivity increases, and connectivity consequently decreases, there is a substantial reduction in link churn; nodes

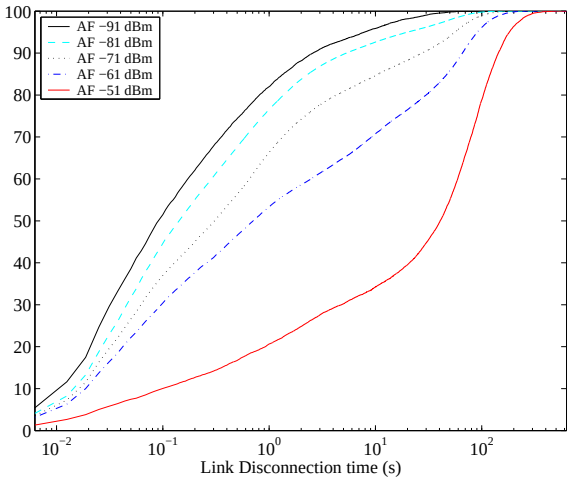

Figure 14: CDF of AF link disconnection times, 40 nodes, CM, Bahen.

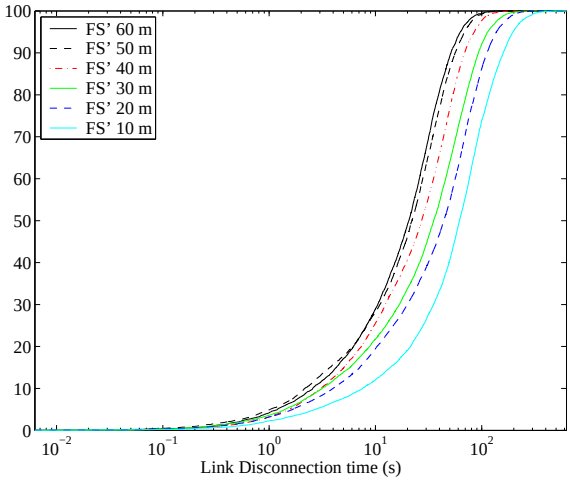

Figure 15: CDF of FS′ link disconnection times, 40 nodes, CM, Bahen.

become less likely to establish weaker links with far away peers, which are more susceptible to experience short disconnections. In contrast, the continuous characteristic of FS propagation results in a different behavior, as illustrated in Figure 15. There are no sudden drops in signal strength, and therefore no intermittent link breakages; the duration of link changes is thus longer than in AF propagation, and the number of link changes significantly lower. Finally, albeit smaller, there is a considerable difference in link changes between CM-FS′ and the other FS′ models. In CM-FS′ nodes move away from each other much more quickly by walking through hallways in opposite directions. In turn, this causes a higher rate of link changes.

DSR does not cope well with the higher rate of link churn in CM-AF. DSR reacts to packet drops (which may result from extremely transient disconnections) by triggering expensive route maintenance cycles; DSR implicitly assumes that once a link goes down, it will remain down for a long period of time. Unfortunately, because most link breakages are actually short-lived, this policy results in gratuitous route discoveries that increase network contention and in turn result in more packet drops. For large networks this cycle can eventually lead to a congestion collapse as illustrated in Figures 7 (c) and 10 (c).

We note that the DSR implementation we used includes mechanisms designed to reduce the rate and cost of route discovery operations, such as route caching, salvaging, and expanding ring search. The low DSR performance under CM-AF suggests that these mechanisms fail to cope with frequent transient disconnections.

DSDV, on the other hand, is less affected by link churn as its periodic and more rigid approach to propagating routing information successfully masks short-lived disconnections. In DSDV, a link is diagnosed as broken only after three periodic updates from the corresponding node have not been received. Moreover, several timing constraints prevent unrestricted propagation of triggered updates, and allow for aggregation of these updates to reduce routing overhead.

6.4 Network Coverage

Figures 16 and 17 show the neighbor density, the average fraction of nodes within transmission range from each other, for networks of 40 nodes in Bahen and Pratt, respectively. These metrics are also normalized to the network size (by dividing by the maximum number of neighbors, i.e. $n-1$), and thus results for networks of 30 and 50 nodes are practically identical and not included. Neighbor density is independent of the communication pattern.

Neighbor density for CM-AF is initially higher than the corresponding values for the FS′-based models. When no obstacles block the primary ray between transmitter and receiver, AF propagation can actually reach farther in obstacle-free areas such as hallways and large conference rooms. However, the situation

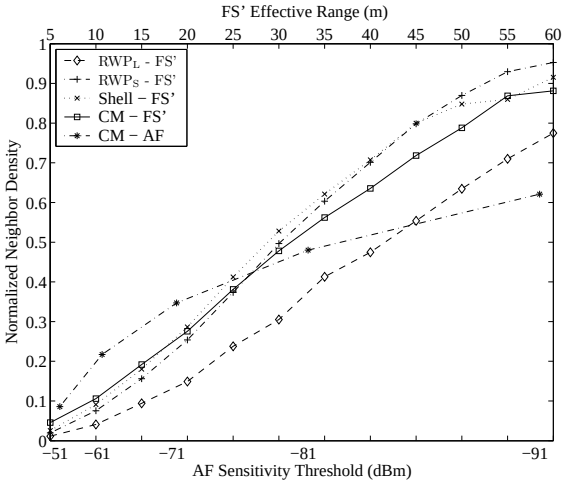

Figure 16: Normalized neighbor density, Bahen

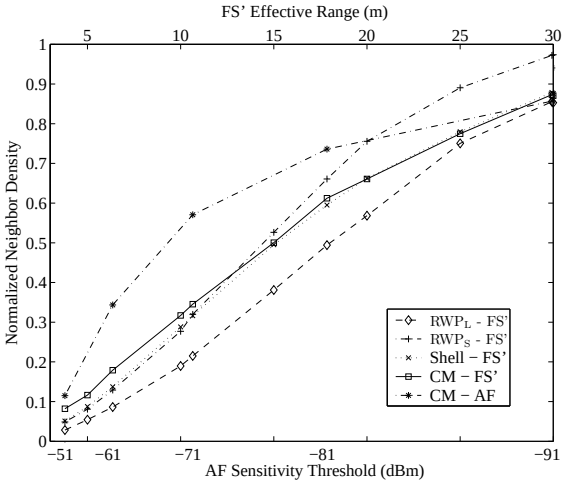

Figure 17: Normalized neighbor density, Pratt.

reverses as transmission power increases and the effects of propagation through multiple walls become the limiting factor in AF propagation. CM-FS′, Shell-FS′ and RWP_S-FS′ have similar neighbor densities. This result suggests that under FS′ propagation, neighbor density is mostly dependent on the effective movement area, as opposed to the specific paths taken by nodes. RWP_L-FS′ models a larger space and consequently has lower neighbor density.

There is a significant difference in the peak neighbor density of CM-AF in Bahen and Pratt. In Pratt, nodes transmitting at full power achieve almost complete coverage of the building (roughly 86 %). The ad hoc network is thus reduced in most cases to a trivial single-hop scenario, and the routing burden is substantially ameliorated. As shown in Figure 9 (c)), the performance of DSR with CM-AF improves abruptly (approximately 40 %) when transmission coverage enables single-hop networking. In contrast, the much larger dimensions of Bahen limit neighbor density to a maximum of 62% and disallow the single-hop case.

7 Discussion and Recommendations

While the CM-AF model is significantly more detailed than the simple models used in mainstream simulators (i.e., RWP_L-FS′), it makes a number of simplifying assumptions, most importantly assuming a time-invariant channel. Therefore, the robustness of CM-AF as a simplification of real-life conditions is not guaranteed. However, given that the simplified models are not robust simplifications of CM-AF in our environment, we postulate that it is very unlikely that they are robust simplifications of real-world environments.

A next possible step would entail verification of our models through actual network deployment. This is very challenging: the logistics and unpredictability of deploying 40 to 50 MANET nodes in an indoor building subject to numerous sources of external noise are overwhelming. The complexity of similar experiments in substantially more benign conditions – outdoor football fields or parking lots – has been well documented [20, 21]. While a small experiment with less than a dozen static nodes is entirely feasible, it will fail to reproduce the conditions under which our simulations have detected poor scalability of routing protocols.

We have pointed out in the introduction that the poor scalability of controlled MANET deployments is one of the major reasons behind the persistence of simulation-based studies. In this light, it is of vital importance to improve the quality of simulation-based studies. We have shown through empirical measurements (for propagation) and construction (for mobility) that our simulation models are firmly acquainted with the real physical characteristics of the environments under study. While the focus of this paper rests on simulation models, we highlight the need for more aggressive validation of the remaining layers of

a simulator: MAC and routing protocols, traffic patterns and behavioral modeling.

We conclude this section by making two recommendations for the design of reactive MANET protocols. These recommendations are based on insight gained from understanding the reasons for DSR's poor performance under high link churn rate (i.e., CM-AF). First, a certain amount of hysteresis should be added when discarding routes; this can prevent the excessive routing effort we have observed under high link change rates. Second, hop-count is known to be a highly misleading metric for the choice of "better" routes: the shortest routes usually employ weak links to distant nodes, which are prone to disconnections. Instead, choosing paths based on signal quality is likely to yield more durable routes.

8 Related Work

Studies on simplified simulation models have focused on the limitations of either the radio propagation or node mobility models considered *individually* [22, 20, 23, 24]. To the best of our knowledge, we are the first group to consider detailed propagation and mobility models *in conjunction*: our preliminary results [25] were presented two years earlier than other work considering the interaction of multiple modeling layers [26]. We are also, to the best of our knowledge, the first to focus on complex indoor environments, to identify robustness as a desirable property of simulation models, and to evaluate this qualitative property for commonly used simplified simulation models. The rest of this section discusses related work on radio and mobility modeling.

8.1 Radio Modeling

There is significant related work on radio propagation models. The *ns2* [16] simulator implements the Two-Ray Ground propagation model, a variation of the Free Space propagation model that considers a second ray reflecting off the ground for long distances. Two-ray Ground is better suited for outdoor environments involving distances longer than a hundred meters. Jardosh et al. [27] experimented with the Line-of-Sight (LOS) model in the context of outdoor propagation. Our experience with LOS show that this propagation model is too restrictive for indoor environments as communication requires nodes to be conveniently placed at hallway intersections. Ray-Tracing is a deterministic technique that models fine-grained radio effects including reflection, diffraction and scattering. Ray-Tracing is extremely computationally expensive, and implementations in the scope of indoor MANET simulation [28] have been limited to very small floor plans. Takai et al. [29] used Ricean and Rayleigh distributions to research small scale fading effects in the context of MANET simulations.

The AF model used in this paper is derived from the Attenuation Factor model proposed by Rappaport and Seidel [7, 8]. A simpler variant of AF, called the Wall Attenuation Factor, was used in the RADAR project for location tracking [9]. To the best of our knowledge, this paper is the first to use the AF model in the context of MANET simulation.

8.2 Mobility Modeling

Most previous on mobility models has focused on outdoor environments. Similar to CM, most enhanced mobility models use a graph to constraint node movement. The City Section Mobility Model [30] uses a bi-dimensional grid to model vehicle movement on city streets in a coarse-grained manner. Tian et al. [31] present a more flexible model in which an arbitrary user-defined graph, corresponding to the layout of the streets in a city, is used to restrict the movement of nodes. The Obstacle Mobility Model (OM) [27] uses automatically-generated Voronoi graphs to model building-to-building movement in a university campus. Jetcheva et al.[32] present an alternative approach which uses actual traces of movements of city buses.

There is little related work on node mobility modes for indoor MANET simulation. Most modeling research focuess on outdoor scenarios or abstract deployment models [33, 34, 35] for which no application to indoor environments has been realized. Johansson et al. [5] considered conference, event coverage, and disaster area scenarios, with a few simple obstacles. Most of the nodes in the simulation are static or have little mobility, and of the scenarios modeled, the conference room is the only indoors one. In CAD-HOC [12], arbitrary obstacles can be placed in a topography, and nodes are allowed to move randomly inside the "empty" areas. The scale of the topography and obstacles can be reduced to fit an indoor scenario, in which case the resulting model will resemble our Shell mobility model. To the best of our knowledge, no mobility model is based on the original specification of an indoor environment. The use of AutoCAD floor plans in CM enables faithful modeling of fine-grained obstacles and significantly more complex indoor environments.

9 Conclusions and future work

We provided the first evaluation of MANET routing protocols in indoor environments using detailed mobility and radio propagation models that account for fine-grained obstacles and building materials.

We showed that simple radio propagation and node mobility models are not robust (at least) for indoor environments, and may lead researchers to reach erroneous conclusions. The simplifications we considered had drastically different effects on the perceived performance of the two protocols used in our

experiment. Even within the same protocol, the effects of simplifications on performance varied erratically between configurations.

These findings raise doubt about the validity of simulation-based MANET evaluations employing simple models. Our experiments indicate that even if a simple model appears to be a good approximation for evaluating a specific MANET protocol, there are no assurances that the model will be valid for other routing protocols, or even the same protocol under different experimental conditions.

We observe that while the effects that different simulation models have on the network topology – measured by metrics such as neighbor density and link changes count – are foreseeable and intuitive, the effects that these changes will in turn have on the performance of routing protocols are extremely hard to predict. We have found that the internals of routing protocols, and the way they react to the topological changes introduced by different simulation models, are complex and often surprising.

The above observations are a compelling indication of the importance of further research on the development and validation of realistic models for indoor MANET simulation.

In the future, we intend to research realistic behavioral models of node mobility in which destinations for node movement are not chosen randomly. We also plan to extend our node mobility and radio propagations models to take into consideration multiple floors and smaller obstacles such as furniture. In the long run, we want to relax the assumption of a time-invariant radio channel and model the effect of human activity, which our empirical measurements showed to be significant.

Acknowledgment

We thank Angela Demke-Brown, Ashvin Goel, Baochun Li, Ben Liang, Peter Marbach, and the students of the systems group for their helpful suggestions. We also thank the SECON 2004 reviewers for their feedback on earlier versions of this manuscript. We also thank Parham Aarabi and Norman Wilson for enabling access to the computing clusters where we ran our simulations. Finally, we express our gratitude to Mary Jane Dundas for setting up the logistics needed to perform field measurements. This research was partially funded by the NSERC Discovery Grant 261545-03. Andrés Lagar Cavilla was partially funded by a Wolfond Scholarship.

References

[1] D. B. Johnson and D. A. Maltz, "Dynamic source routing in ad hoc wireless networks," in *Mobile Computing* (Imielinski and Korth, eds.), vol. 353, Kluwer Academic Publishers, 1996.

[2] C. Perkins and P. Bhagwat, "Highly dynamic destination-sequenced distance-vector routing (DSDV) for mobile computers," in *Proceedings of ACM SIGCOMM'94 – Conference on Communications Architectures, Protocols and Applications*, (London, UK), pp. 234–244, Aug. - Sept. 1994.

[3] C. E. Perkins and E. M. Royer, "Ad hoc on demand distance vector routing," in *Proceedings of WMCSA '99 – 2nd IEEE Workshop on Mobile Computing Systems and Applications*, (New Orleans, LA), pp. 90–100, Feb. 1999.

[4] J. Broch, D. A. Maltz, D. B. Johnson, Y.-C. Hu, and J. Jetcheva, "A performance comparison of multi-hop wireless ad hoc network routing protocols," in *Proceedings of MobiCom '98 – Fourth Annual International Conference on Mobile Computing and Networking*, (Dallas, TX), pp. 85–97, Oct. 1998.

[5] P. Johansson, T. Larsson, N. Hedman, B. Mileczarek, and M. Degermark, "Scenario-based performance analysis of routing protocols for mobile ad-hoc networks," in *Proceedings of MobiCom '99 – 5th annual ACM/IEEE international conference on Mobile Computing and Networking*, (Seattle, WA), pp. 195–206, Aug. 1999.

[6] S. R. Das, C. E. Perkins, and E. E. Royer, "Performance comparison of two on-demand routing protocols for ad hoc networks," in *Proceedings of INFOCOM '00 – IEEE Conference on Computer Communications*, vol. 1, (Tel-Aviv, Israel), pp. 3–12, Mar. 2000.

[7] T. S. Rappaport, *Wireless Communications: Principles & Practice*. Prentice Hall, 2002.

[8] S. Y. Seidel and T. S. Rappaport, "Site-specific propagation prediction for wireless in-building personal communication system design," *IEEE Transactions on Vehicular Technology*, vol. 43, pp. 879–891, Apr. 1994.

[9] P. Bahl and V. N. Padmanabhan, "RADAR: An in-building RF-based user location and tracking system," in *Proceedings of INFOCOM '00 – IEEE Conference on Computer Communications*, vol. 2, (Tel-Aviv, Israel), pp. 775–784, Mar. 2000.

[10] "Superpass SPDG80-D3 antenna specifications sheet." `http://www.superpass.com/SPDG80-D3.html`.

[11] "Enterasys RoamAbout wireless high-rate pc card." `http://www.enterasys.com/products/wireless/CSIxD-AA/`.

[12] S. Shah, E. Hernandez, and A. S. Helal, "Cad-hoc: A cad like tool for generating mobility benchmarks in ad-hoc networks," in *Proceedings of SAINT '02 – Symposium on Applications and the Internet*, (Nara City, Japan), pp. 270–280, Jan.–Feb. 2002.

[13] A. P. Jardosh, E. M. Belding-Royer, K. C. Almeroth, and S. Suri, "Real-world environment models for mobile network evaluation." To appear in Journal on Selected Areas in Communications, special issue on Wireless Ad Hoc Networks, 2005.

[14] S. Ray, "Realistic mobility for manet simulation," Master's thesis, University of British Columbia, 2003.

[15] T. H. Cormen, C. E. Leiserson, and R. L. Rivest, *Introduction to Algorithms*. MIT Press, 1990.

[16] N. Drakos and R. Moore, *ns2 - The Manual (formerly Notes and Documentation)*, 1999.

[17] "The Monarch Project." `http://www.monarch.cs.rice.edu`.

[18] H. A. Lagar Cavilla, "MANET extensions to ns2." `http://www.cs.toronto.edu/~andreslc/software/MANET_extensions.tgz`.

[19] J. Yoon, M. Liu, and B. Noble, "Random waypoint considered harmful," in *Proceedings of INFOCOM '03 – IEEE Conference on Computer Communications*, vol. 2, (San Francisco, CA), pp. 1312–1321, May–Apr. 2003.

[20] J. Liu, Y. Yuan, D. M. Nicol, R. S. Gray, C. C. Newport, D. Kotz, and L. F. Perrone, "Simulation validation using direct execution of wireless ad-hoc routing protocols," in *Proceedings of PADS – Workshop on Parallel and Distributed Simulation*, (Kufstein, Austria), pp. 7–16, May 2004.

[21] D. A. Maltz, J. Broch, and D. B. Johnson, "Quantitative lessons from a full-scale multi-hop wireless ad hoc network testbed," in *Proceedings of WCNC 2000 – IEEE Wireless Communications and Networking Conference*, vol. 3, (Chicago, IL), pp. 992 – 997, Sept. 2000.

[22] J. Heidemann, N. Bulusu, J. Elson, C. Intanagonwiwat, K. Lan, Y. Xu, W. Ye, D. Estrin, and R. Govindan, "Effects of detail in wireless network simulation," in *Proceedings of the SCS Multiconference on Distributed Simulation*, (Phoenix, AZ), pp. 3–11, Jan. 2001.

[23] M. Takai, J. Martin, and R. Bagrodia, "Effects of wireless physical layer modeling in mobile ad hoc networks," in *Proceedings of MobiHoc '01 – Second ACM Symposium on Mobile Ad Hoc Networking and Computing*, (Long Beach, USA), pp. 87–94, Oct. 2001.

[24] M. Bhatt, R. Chokshi, S. Desai, S. Panichpapiboon, N. Wisitpongphan, and O. Tonguz, "Impact of Mobility on the Performance of Ad-hoc Wireless Networks," in *Proc. of the IEEE Vehicular Technology Conference (VTC)*, 2003.

[25] A. Lagar Cavilla, G. S. Baron, T. E. Hart, L. Litty, and E. de Lara, "Simplified simulation models for indoor manet evaluation are not robust," in *Proceedings of the First IEEE Conference on Sensor and Ad-Hoc Communications and Networks*, Oct. 2004.

[26] J. M. Dricot, P. De Doncker, and E. Zimnyi, "Multivariate Analysis of the Cross-Layer Interaction in Wireless Network Similulations," in *Proc. of*

International Workshop on Wireless Ad-hoc Networks (IWWAN), (London, UK), May 2005.

[27] A. Jardosh, E. M. Belding-Royer, K. C. Almeroth, and S. Suri, "Towards realistic mobility models for mobile ad hoc networks," in *Proceedings of MobiCom '03 – Ninth Annual International Conference on Mobile Computing and Networking*, (San Diego, CA), pp. 217–229, Sept. 2003.

[28] J.-M. Dricot and P. D. Doncker, "High accuracy physical layer models for wireless network simulations in ns-2," in *Proceedings of IWAN '04 – International Workshop on Wireless Ad-hoc Networks*, (Oulu, Finland), May–June 2003.

[29] M. Takai, R. Bagrodia, K. Tang, and M. Gerla, "Efficient wireless network simulations with detailed propagation models," *Wireless Networking*, vol. 7, no. 3, pp. 297–305, 2001.

[30] V. Davies, "Evaluating mobility models within an ad hoc network," Master's thesis, Colorado School of Mines, 2000.

[31] J. Tian, J. Hahner, C. Becker, I. Stepanov, and K. Rothermel, "Graph-based mobility model for mobile ad hoc network simulation," in *Proceedings of the 35th Annual Simulation Symposium*, (San Diego, USA), pp. 337–344, Apr. 2002.

[32] J. G. Jetcheva, Y.-C. Hu, S. PalChaudhuri, A. K. Saha, and D. B. Johnson, "Design and evaluation of a metropolitan area multitier wireless ad hoc network architecture," in *Proceedings of WMCSA '03 – 5th IEEE Workshop on Mobile Computing Systems and Applications*, (Monterey, CA), pp. 9–10, Oct. 2003.

[33] T. Camp, J. Boleng, and V. Davies, "A survey of mobility models for ad hoc network research," *Wireless Communications & Mobile Computing (WCMC): Special issue on Mobile Ad Hoc Networking: Research, Trends and Applications*, vol. 2, no. 5, pp. 483–502, 2002.

[34] C. Bettstetter, "Mobility modeling in wireless networks: categorization, smooth movement, and border effects," *ACM SIGMOBILE Mobile Computing and Communications Review*, vol. 5, pp. 55–66, July 2001.

[35] C. Bettstetter and C. Wagner, "The spatial node distribution of the random waypoint mobility model," in *Proc. 1st German Workshop on Mobile Ad-Hoc Networks (WMAN'02), Ulm, Germany*, pp. 41–58, 2002.